First publ. in: Physical Review Letters 86 (2001), 8, pp. 1630-1633

Mechanisms for the Generation of Coherent Longitudinal-Optical Phonons in GaAs/AlGaAs Multiple Quantum Wells

K. J. Yee,[1] Y. S. Lim,[2] T. Dekorsy,[3] and D. S. Kim[1,*]

[1]*Department of Physics, Seoul National University, Seoul 151-742, Korea*
[2]*Department of Applied Physics, Konkuk University, Chungju, Chungbook 380-701, Korea*
[3]*Institut für Ionenstrahlphysik und Materialforschung, FZ Rossendorf, D-01314 Dresden, Germany*

We show that coherent optical phonons in GaAs multiple quantum wells are generated in a completely different way as compared to bulk GaAs. Unlike in bulk GaAs where the ultrafast screening of electric fields by photogenerated charge carriers is known to be dominant, three distinctive generation mechanisms contribute simultaneously in multiple quantum wells. The interplay between impulsive Raman scattering, forbidden Raman scattering, and screening of surface electric fields, whose relative strengths are determined by laser intensity, detuning from the exciton resonance, and the barrier width, generates a rich variety of new phenomena.

With the advent of ultrashort pulse lasers, the generation and detection of coherent lattice vibrations in various crystals became possible [1–8]. Recently, terahertz radiation from coherent phonons, coherent control of coherent phonons, and large amplitude coherent acoustic phonons have been studied [9–11]. In addition, coherent phonon oscillations have been proposed as an effective femtosecond x-ray switch [12]. Despite these activities, however, the generation mechanism of coherent phonons is still not completely understood even in bulk materials.

In bulk GaAs, it is generally agreed that screening of the surface field by carriers generated by femtosecond laser pulses is responsible for the coherent phonon generation [8]. In semimetals such as Bi, Te, and Sb, the so-called displacive excitation of coherent phonons (DECP) was proposed [2]. However, it was later shown that these results can also be accounted for by resonant stimulated Raman scattering [13,14]. Both the screening mechanism in GaAs and the DECP mechanism in semimetals are "displacive" in nature, and the phonon oscillation is then "cosinelike." In general, materials which exhibit displacive generation mechanisms are opaque at the laser photon energies used. On the other hand, in transparent materials, impulsive stimulated Raman or Brillouin scattering (ISRS or ISBS) have been established as the coherent phonon generation mechanism [15,16]. These mechanisms are "impulsive" in nature and thus have "sinelike" oscillation.

In GaAs multiple quantum wells, the electronic intersubband energy separation relative to the optical phonon energy has been proposed as an important factor in determining the screening of coherent phonon oscillations [17]. In superlattices, coherent acoustic phonons have been found to be excited via an impulsive Raman process [18]. However, there have been no prior studies on how exactly coherent longitudinal-optical (LO) phonons are generated in multiple quantum wells.

In this Letter, we study the generation mechanism of coherent LO phonons in GaAs/AlGaAs quantum well structures. We find that near the exciton resonance, the interference between the impulsive allowed and forbidden Raman scatterings dominate coherent phonon generation. This is in stark contrast to bulk GaAs, where the impulsive stimulated Raman scattering makes little contribution. As intensity, temperature, detuning, and sample parameters vary, screening also contributes. It is interesting to note that both the impulsive and the displacive mechanisms may contribute simultaneously. Therefore, our experiments shed important insight on the generation mechanisms of coherent phonons in general: even for opaque materials, impulsive Raman scattering can contribute significantly, depending on how close the laser photon energy is to resonance, sample temperature, and excitation density.

Using femtosecond laser pulses, we perform reflective electro-optic sampling (REOS) on bulk GaAs, $GaAs/Al_{0.36}Ga_{0.64}As$ multiple quantum wells (MQW's) and superlattices (SL's). A Kerr-lens mode-locked Ti:sapphire laser was employed to generate transform-limited pulses of ~50 fs duration. All samples were grown on (001)-GaAs substrates by the molecular-beam-epitaxy technique. The MQW sample mostly investigated in our study has a 15 nm well width, 5 nm barrier width, and 30 periods. We also studied samples with identical parameters except for the barrier widths of 3, 2, and 1 nm. With the polarization of the probe beam fixed parallel to one of the principal axes ([100], [010]), the pump beam polarization was rotated to characterize the polarization dependence of the coherent phonon oscillations.

Figure 1(a) is the REOS signals in time domain showing oscillations at the LO phonon frequency, obtained at the pump intensity of I_0 (= 200 MW/cm^2) and at 12 K for the MQW sample of $L_b = 5$ nm, with pump beam polarizations parallel to the [110], [100], [1$\bar{1}$0] crystal axes and at an angle corresponding to the minimum of the phonon amplitude. I_0 corresponds approximately to the sheet density of 4×10^{11} cm^{-2} and the photon energy was roughly centered at the heavy hole exciton resonance.

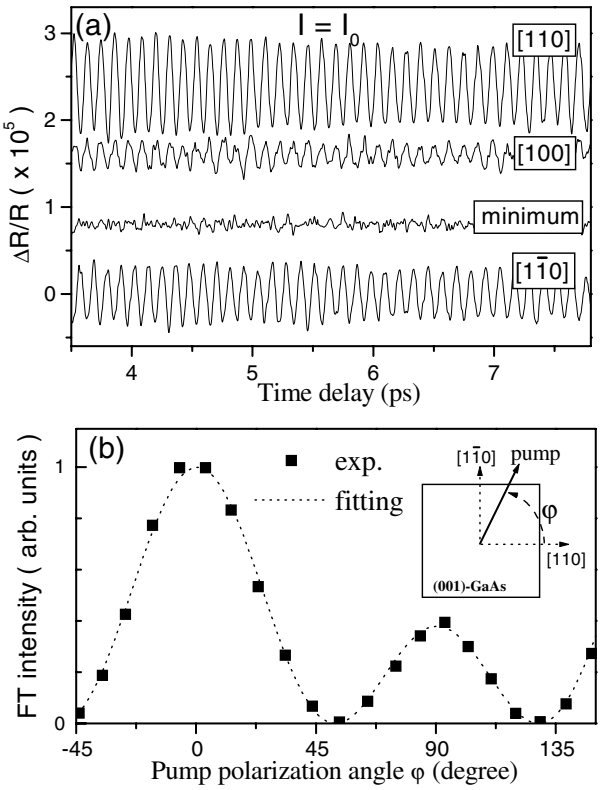

FIG. 1. (a) Coherent phonon oscillations for the $GaAs/Al_{0.36}Ga_{0.64}As$ MQW with barrier width (L_b) = 5 nm, with center wavelength slightly above the $n = 1$ exciton resonance, and at pump intensity of I_0 (= 200 MW/cm^2). Pump beam polarizations are parallel to the [110], [100], [1$\bar{1}$0] crystal axes or at "minimum" at which the phonon oscillation is minimum. (b) The Fourier-transformed intensity as a function of the polarization angle φ of the pump beam. Dotted lines result from the fitting; φ is defined as an angle from the [110] crystal axis as in the inset.

Figure 1(b) shows Fourier-transformed intensity of the coherent phonon oscillations as a function of the polarization angle φ of the pump beam. As is depicted in the inset, φ is defined as an angle measured from the [110] crystal axis. A strong dependence on the pump polarization is evident and the maxima appear at the [110] and [1$\bar{1}$0] directions. The oscillation is much suppressed around the [100] direction but note that the "minimum" angle does not coincide with the [100] direction but deviates by about 5° from it. Another salient feature is that there exists an apparent asymmetry between the [110] and the [1$\bar{1}$0]. This behavior is in stark contrast to the previous report on bulk GaAs where virtually no polarization dependence was observed [8]. We note that even at resonant excitation condition at low temperature there is little angle dependence for bulk GaAs.

From the above observations, it is clear that the dominant generation mechanism is not screening of electric fields in the MQW. This effect would depend only on the absolute number of generated carriers and is thus independent of the pump polarization. In order to explain the polarization dependence, we note that in the impulsive stimulated Raman scattering, one spectrally broad femtosecond pulse provides both the exciting photon and the Raman-stimulated photon [15]. In other words, both the incoming and outgoing photon polarization that "surround" the Raman tensor are the same. Including both the deformational potential interaction and the first order electro-optic effect, the allowed Raman tensor (R_A) of the (001)-GaAs is given as follows for the backscattering geometry along the [001] direction:

$$R_A = \begin{pmatrix} 0 & a \\ a & 0 \end{pmatrix}, \tag{1}$$

where a is the Raman polarizability. The scattering efficiency of the ISRS for this configuration is then given by $a^2 \times \cos^2(2\varphi)$. This partially explains the angle dependence shown in Fig. 1(b) but not the asymmetry, nor the fact that the minimum is not at $\varphi = 45°$. These discrepancies can be removed, if we introduce the "forbidden," q-dependent Fröhlich interaction amplitude and consider its interference with the "allowed," deformation interaction term [19,20]. The Fröhlich term is zero in the dipole approximation ($q = 0$), and thus called "forbidden," but is stronger than the allowed deformation potential terms under some resonant conditions. Including this term which is diagonal, the matrix becomes

$$R_{\text{total}} = \begin{pmatrix} b & a \\ a & b \end{pmatrix}, \tag{2}$$

where b is the Raman polarizability of the Fröhlich interaction. With the pump polarization angle φ defined earlier, the scattering intensity as a function of the angle is then

$$\frac{dS}{d\Omega} \propto |b + a \times \cos(2\varphi)|^2 + c^2. \tag{3}$$

Note that in Eq. (3), we included the angle-independent term c^2 which is due to the screening of the field, for the sake of generality. This model fits the angular dependence very well with parameters $b/a = 0.24$ and $c/a = 0$, as shown in Fig. 1(b) as dotted lines. The two Raman amplitudes a and b interfere constructively in the [110] direction and destructively in the [1$\bar{1}$0] direction. Here, the two complex values a and b are nearly of the same phase, because the minimum phonon intensity is nearly zero.

We now show that, as the laser intensity increases, screening of the surface field begins to contribute. Figure 2(a) shows the coherent phonon oscillations at the pump intensity of $2I_0$ for the MQW, and the angle dependence of the Fourier-transformed intensity is shown in Fig. 2(b). At this intensity, the coherent phonon amplitude is not negligible even at the minimum angle. This behavior cannot be explained by the impulsive Raman mechanisms only, but introducing the displacive screening mechanism as in Eq. (3) can nicely resolve it, as shown in Fig. 2(b) as dotted lines. The fitting parameters are $b/a = 0.16$ and $c/a = 0.29$. It should also be noted that there exists approximately a 90° phase difference between the minimum

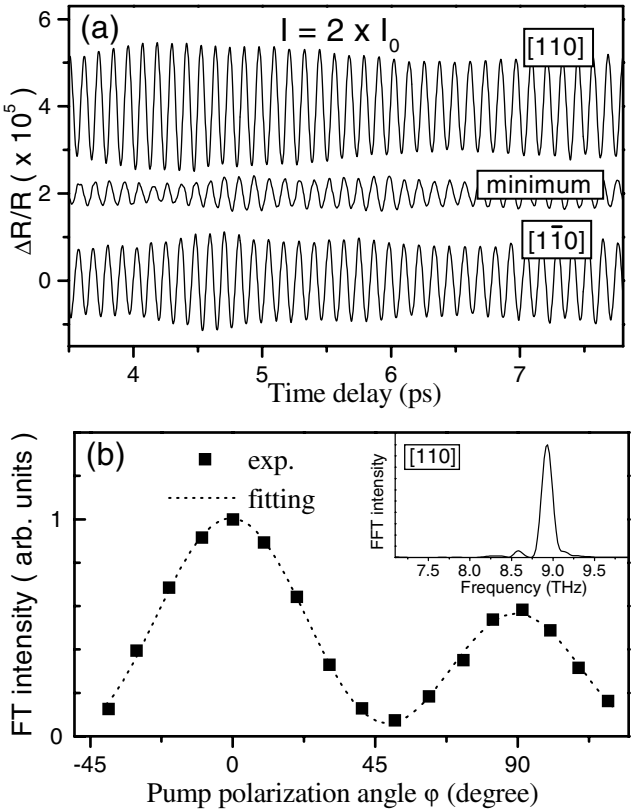

FIG. 2. (a) Coherent optical phonon oscillations in the time domain at higher pump intensity of $2I_0$ obtained for the MQW with $L_b = 5$. (b) The Fourier-transformed intensity as a function of the polarization angle φ of the pump beam. Dotted lines result from the fitting with parameters $b/a = 0.16$ and $c/a = 0.29$. The inset is the Fourier-transformed spectrum for a typical oscillation.

oscillation and the maximum oscillations. This supports that at the minimum oscillation angle, the generation of coherent phonons is dominated by screening. We also note that raising the temperature has a similar effect, i.e., a decrease in the Raman nonlinearity due to the broadening of the exciton resonance that relatively favors the screening contributions. The inset in Fig. 2(b) shows the Fourier-transformed spectrum for a typical oscillation. A minor peak at 0.35 THz below the main GaAs LO phonon is possibly due to the GaAs-like LO mode in the barrier, but further studies are needed [21].

In Fig. 3, we show several periods of oscillations at pump intensities of I_0 and $2I_0$ with the pump polarization parallel to [110] or [1$\bar{1}$0] directions. A phase shift of about π exists at both I_0 and $2I_0$ between these two directions. It is interesting that for $I = 2I_0$, the phase difference deviates noticeably from π. This can also be explained in our model as shown by the dotted lines, with the same fitting parameters used in Figs. 1(b) and 2(b). Note that the phase shift between $\pm a \times \sin\Omega t + c \times \cos\Omega t$ is not π unless c is zero.

The fact that both the angle and the time dependence of the coherent phonon oscillation are explained simultaneously gives strong evidence for the validity of our model. In order to further support the model for the coherent phonon generation process in MQW, we tuned the laser energy. Figure 4 shows the Fourier-transformed intensity as a function of pump polarization when the excitation energy is slightly above the $n = 2$ heavy hole exciton. The behavior reveals a striking deviation from the angle dependence at the $n = 1$ resonance shown in Fig. 1(b). The [1$\bar{1}$0] direction is now a minimum instead of a maximum, and the angle-independent component makes the strongest contribution. Fitting the angular dependence with Eq. (3), we obtain the parameters $b/a = 1.4$, $c/a = 3.4$ (dotted lines, Fig. 4). For this condition, the dominant generation mechanism is proved to be the screening. We note that free carrier screening becomes more effective when the excess energy is large.

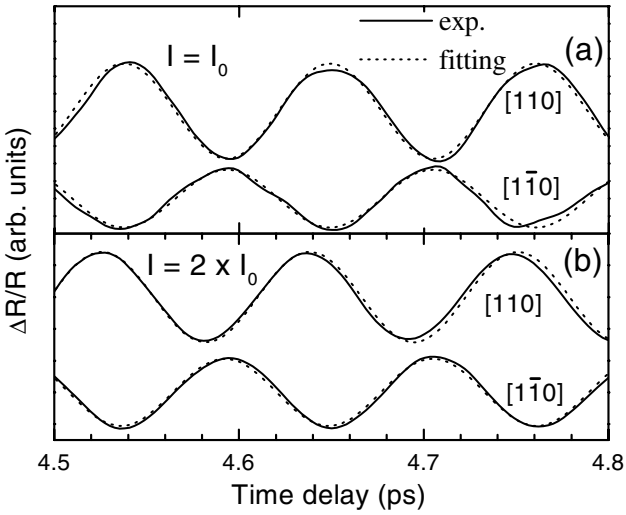

FIG. 3. Several periods of phonon oscillations at pump intensity of I_0 (a) and $2I_0$ (b) for the MQW with $L_b = 5$ nm (solid lines). The fittings (dotted lines) were obtained with the same b/a and c/a, obtained from the fittings in Fig. 1(b) and in Fig. 2(b).

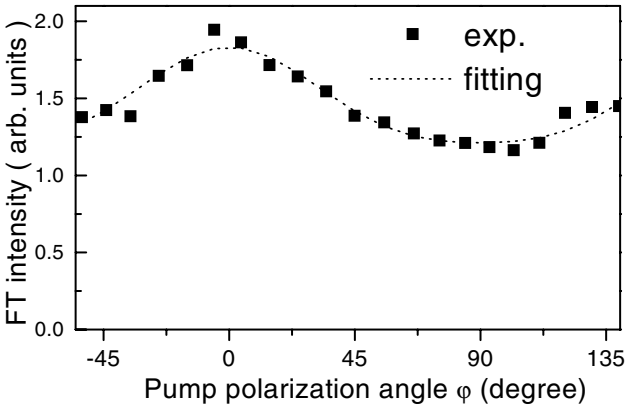

FIG. 4. Fourier-transformed intensity with the excitation energy slightly above the $n = 2$ subband energy. Dotted lines are fittings of Eq. (3) with $b/a = 1.4$ and $c/a = 3.4$.

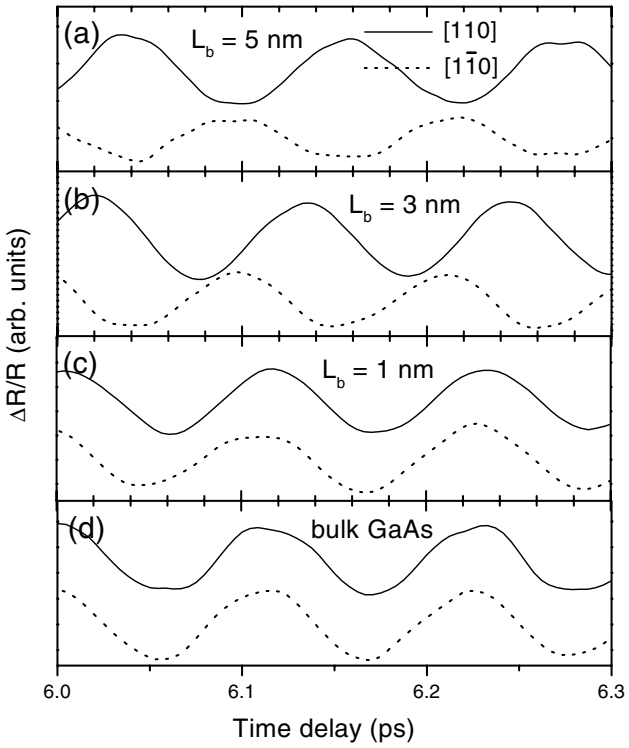

FIG. 5. Several periods of phonon oscillations for the MQW with (a) $L_b = 5$ nm, (b) $L_b = 3$ nm, (c) $L_b = 1$ nm, and (d) for a bulk GaAs, respectively, with pump polarizations parallel to [110] (solid lines) or [1$\bar{1}$0] (dotted lines) crystal axes.

To further test our model, we performed our experiments on SL's with the barrier widths of 1 or 3 nm, with fixed well width of 15 nm. For these thin barrier structures, well-to-well coupling exists across the thin barriers, and the carriers are not confined within each well [22,23]. Eventually, for thin enough barriers, bulklike generation of coherent phonons should become possible. We show in Fig. 5 coherent LO phonon oscillations at the [110] and [1$\bar{1}$0] polarizations for these thin barrier structures together with those for the MQW with $L_b = 5$ nm. Laser center energies were tuned at the heavy-hole exciton for each sample. The phase shift between the two polarization configurations becomes smaller as the barrier becomes thinner, and at the barrier width of 1 nm, virtually no angle dependence is found, just as in bulk GaAs. Figure 5, therefore, is a manifestation of MQW-to-SL transition of the coherent LO phonon generation: coherent phonons are generated by impulsive Raman scattering in MQW, while screening becomes more and more important as the barrier becomes thinner, eventually overriding other generation mechanisms.

In conclusion, we have shown that the impulsive stimulated Raman scattering, both allowed and forbidden, and electric field screening give the complete description of the coherent phonon generation in GaAs multiple quantum wells, including both phase and amplitude of the oscillations. Intensity, temperature, detuning, and barrier-width dependencies of the relative contributions of the three generation mechanisms result in a rich variety of physics.

We acknowledge helpful discussions with D. S. Yee and Y. D. Jho. This work was supported by MOST (the National Research Laboratory Program) and KOSEF (the Center for Strongly Correlated Materials Research, and Grant No. 97-0702-03-01-3).

*Email address: denny@phya.snu.ac.kr

[1] G. C. Cho *et al.,* Phys. Rev. Lett. **65**, 764 (1990).
[2] H. J. Zeiger *et al.,* Phys. Rev. B **45**, 768 (1992).
[3] A. V. Kuznetsov and C. J. Stanton, Phys. Rev. Lett. **73**, 3243 (1994).
[4] A. Yamamoto *et al.,* Phys. Rev. Lett. **73**, 740 (1994).
[5] R. Merlin, Solid State Commun. **102**, 207 (1997).
[6] A. Leitenstorfer *et al.,* Phys. Rev. Lett. **82**, 5140 (1999).
[7] A. Leitenstorfer *et al.,* Phys. Rev. B **61**, 16 642 (2000).
[8] T. Dekorsy *et al.,* in *Light Scattering in Solids VIII,* edited by M. Cardona and G. Guintherodt (Springer, Berlin, 2000).
[9] T. Dekorsy *et al.,* Phys. Rev. Lett. **74**, 738 (1995).
[10] M. Hase *et al.,* Appl. Phys. Lett. **69**, 2474 (1996).
[11] C. K. Sun *et al.,* Appl. Phys. Lett. **75**, 1249 (1999).
[12] P. H. Bucksbaum and R. Merlin, Solid State Commun. **111**, 535 (1999).
[13] G. A. Garrett *et al.,* Phys. Rev. Lett. **77**, 3661 (1996).
[14] T. E. Stevens *et al.,* Phys. Status Solidi (b) **215**, 81 (1999).
[15] Y. X. Yan *et al.,* J. Chem. Phys. **85**, 5391 (1985).
[16] Y. Liu *et al.,* Phys. Rev. Lett. **75**, 334 (1995).
[17] T. Dekorsy *et al.,* Phys. Rev. B **53**, 1531 (1996).
[18] A. Bartels *et al.,* Phys. Rev. Lett. **82**, 1044 (1999).
[19] Jose Menendez and Manuel Cardona, Phys. Rev. Lett. **51**, 1297 (1983).
[20] W. Kaushke *et al.,* Phys. Rev. B **36**, 9129 (1987).
[21] D. S. Kim *et al.,* Phys. Rev. Lett. **68**, 1002 (1992).
[22] G. Bastard, in *Wave Mechanics Applied to Semiconductor Heterostructures* (Halsted, New York, 1988).
[23] K. J. Yee *et al.,* Phys. Rev. B **60**, R8513 (1999).